INTERNATIONAL JOURNAL OF ENERGY RESEARCH, VOL. 15, 203–221 (1991)

SPOUTED AND SPOUT-FLUID BED COMBUSTORS 2: BATCH COMBUSTION OF CARBON

S. TIA, S. C. BHATTACHARYA AND P. WIBULSWAS
Energy Technology Division, Asian Institute of Technology, GPO Box 2754, Bangkok, Thailand

SUMMARY

A batch combustion model of carbon particles in a spouted bed has been developed based on the concept of carbon residence time in each region of the spouted bed (annulus, spout and fountain). Both isothermal and nonisothermal particles are considered, with the assumption of no temperature gradient inside the particle. Model predictions in terms of carbon conversion and burnout time were in good agreement with experimental data obtained from a laboratory scale spouted bed combustor. For comparison, an experimental study on a spout-fluid mode was also carried out.

KEY WORDS Carbon combustion Spouted bed combustor

INTRODUCTION

Spouted beds (SB) and spout-fluid beds (SFB) can be used satisfactorily for burning coal (Lim *et al.*, 1988). The major advantages of an SB or an SFB over a fluidized bed (FB) are the possibility of handling larger and stickier particles (Zhao *et al.*, 1987*a*). However, the fundamental studies on coal combustion in SBs and SFBs are still in the early stage. Khoe and Weve (1983) reported the modes and flow regimes of SB gas combustion. Recently, SFB flow regimes for the intermediate temperature range have been investigated and reported by Zhao *et al.* (1987*a*). Kumpinsky and Amundson (1984) proposed a model for char combustion in an SB of sand, ignoring combustion in the fountain. The model, which considers axial as well as radial variation of reactant concentration, constitutes the closest description of the true reactor behaviour. They pointed out that the lack of information on the solid circulation rate in the bed led to the impossibility of generating models which can follow a particle path from the instant it is injected into the reactor until the time it is burnt out or elutriated. Zhao *et al.* (1987*b*) proposed a simple model for coal burnout time in an SB combustor. The time required for heat-up and devolatilization of a coal particle, as well as the time spent by particles in the spout and fountain regions, are neglected. Assuming that the char temperature was 150 K higher than the measured mean bed temperature, the prediction results were in good agreement with the measured values. Moreover, the measured burnout time in the SB were somewhat shorter than those measured for an FB under comparable conditions. This may be, as suggested by them, due to (i) the decrease in mass transfer resistance because of the high interstitial gas velocities and the absence of bubble phase in the annulus, and (ii) the shedding of ash layer by the energetic shear and collisions in the spout and fountain regions reducing the ash diffusion resistance. Since the attrition rate in an SB is expected to be higher than in an FB, the carbon loss should also be higher; this in turn would also tend to shorten the burnout time.

However, the ignorance of combustion in the spout and fountain regions in the Zhao *et al.* (1987*b*) model can lead to overprediction of coal burnout times for the large coal particles because of the significant decrease in particle residence time in the annulus (Tia, 1990); the residence times in the spout and fountain regions then become longer, and combustion in these regions become more significant.

This paper describes a carbon combustion model for an SB combustor. Both constant and varied carbon particle temperature during combustion are considered, with the assumption of no temperature gradient

0363–907X/91/030203–19$09.50

Received 14 June 1990
Revised 20 September 1990

inside the particle. The model accounts for the combustion in both the spout and fountain regions by considering particle residence times in these regions. The prediction results are compared with those of experiments performed by burning small batches of pyrolysed electrode carbon particles in a laboratory scale sand spouted bed. Off-gas analysis is used to detect the degree of carbon conversion.

MODEL DEVELOPMENT

The development of the batch combustion model of carbon in an SB is based on the following assumptions:

(*a*) In an SB, a carbon particle undergoes a cyclical movement from the annulus to the spout and the fountain, and then falls back again to the annulus (Tia, 1990). It is assumed that the mean cycle time depends only on the diameter of the carbon particle.
(*b*) The bed is isothermal.
(*c*) The oxygen concentration is equal throughout the bed owing to the small batch mass used in the experiment.
(*d*) The spout diameter is constant along the bed height.
(*e*) The combustion mechanism of carbon is based on Model 2 reported by Ross (1979). This model assumes that the carbon is oxidized to form CO at the particle surface, and this is followed by the rapid gas phase combustion of CO near the surface. The overall reaction is effectively $C + O_2 \rightarrow CO_2$. Moreover, the intrinsic combustion reaction is assumed to be first-order.
(*f*) The shape of the carbon particles is spherical.
(*g*) No temperature gradient exists inside a carbon particle. This assumption is supported by the theoretical analysis of Luss and Amundson (1969) and the experiments on particle temperature measurement (Tia, 1990).
(*h*) Since the attrition in an SB is high, and the carbon used in the experiment has a low ash content, the shrinking unreacted particle with constant density can be assumed during the combustion.

After being dropped into the bed, a small batch of N particles of carbon having initial diameter D_{po}, and density ρ_p starts to travel from the annulus surface downward, and then gets entrained into the spout and the fountain. The average residence times spent by the carbon particle in the annulus, spout, and fountain regions are t_a, t_s, and t_f, respectively. The overall oxygen balance, therefore, can be written as

$$-N\pi\rho_p\frac{D_p^2}{24}\frac{dD_p}{dt} = UA_cC_o - UA_cC_e \tag{1}$$

where U is the superficial velocity of air through the combustor, C_o and C_e are the oxygen concentration at combustor inlet and outlet, respectively, and A_c is the cross-sectional area of combustor column. From assumption (*c*), equation (1) becomes

$$-N\pi\rho_p\frac{D_p^2}{24}\frac{dD_p}{dt} = UA_c(C_o - C_b) = Q(C_o - C_b) \tag{2}$$

where Q is the inlet volumetric air flow rate, and C_b is the bed oxygen concentration.

(i) Isothermal particle model

In this model each carbon particle is assumed to have uniform and constant temperature throughout the burning period. The combustion rate of a carbon particle can therefore be expressed as

$$-\pi\rho_p\frac{D_p^2}{24}\frac{dD_p}{dt} = 2\pi D_p^2 k_c C_R = 2\pi D_p \mathrm{Sh}_b D_g(C_b - C_R) = 2\pi D_p^2 K C_b \tag{3}$$

$$\frac{1}{K} = \frac{\omega}{k_c} + \frac{\lambda D_p}{\mathrm{Sh}_b D_g} \tag{4}$$

where K = overall reaction rate constant, k_c = reaction rate constant, C_R = oxygen concentration at particle surface, Sh_b = mean Sherwood number in an SB, D_g = diffusivity of oxygen gas, and ω and λ are constants depending on the combustion mechanism, and in this case both are equal to 2 (assumption (*d*)), above.

Because of the cyclical movement of the carbon particle, the mass transfer of oxygen to the carbon particle surface per unit area during one cycle time is

$$N_{ob}t_c = N_{oa}t_a + N_{os}t_s + N_{of}t_f \tag{5}$$

where N_{oi}, with $i = b, a, s,$ or f, represents the average oxygen mass transfer rate per unit carbon surface area inside the bed, annulus, spout, and fountain regions, respectively. It can be expressed in the form of the Sherwood number as follows:

$$N_{oi} = \frac{\mathrm{Sh}_i D_g t_i}{D_p}(C_i - C_R), \quad i = b, a, f, s \tag{6}$$

Since it is assumed that the oxygen concentrations in all the regions of the SB are equal, from equations (5) and (6) and the definition of probability of carbon particle defined in Part 1 of this paper (Tia *et al.*, 1991*b*), the mean Sherwood number in an SB is

$$\mathrm{Sh}_b = p_a\mathrm{Sh}_a + p_f\mathrm{Sh}_f + (1 - p_a - p_f)\mathrm{Sh}_s \tag{7}$$

The Sherwood number for a single particle in both the spout and the fountain regions, can, owing to their high voidage, be approximated from the correlation of Ranz and Marshall (1952). So

$$\mathrm{Sh}_i = 2 + 0{\cdot}69\mathrm{Re}_i^{1/2}\mathrm{Sc}^{1/3}, \quad i = s, f \tag{8}$$

Since the annulus voidage is nearly the same as that of the emulsion phase of an FB, the Sherwood number proposed by La Nauze and Jung (1982) is used:

$$\mathrm{Sh}_a = 2\varepsilon_a + 0{\cdot}69\mathrm{Re}_a^{1/2}\mathrm{Sc}^{1/3} \tag{9}$$

Substituting equations (7)–(9) into equation (3), and then using equation (2), it can be shown after some rearrangement that

$$-\frac{dD_p}{dt} = \left[\frac{N\pi\rho_p D_p^2}{24QC_o} + \frac{\rho_p}{24C_o k_c} + \frac{D_p}{A + BD_p^{1/2}}\right]^{-1} \tag{10}$$

$$A = \frac{48D_gC_o}{\rho_p}[p_a\varepsilon_a + p_f + (1 - p_a - p_f)]$$

$$B = \frac{16{\cdot}56D_gC_o\mathrm{Sc}^{1/3}}{\rho_p v_g^{1/2}}[p_a(u_a + v_a)^{1/2} + p_f u_f^{1/2} + (1 - p_a - p_f)(u_s - v_s)^{1/2}]$$

Integration of equation (10) from $t = 0$ to $t = t$ yields

$$t = \frac{2}{3B}D_{po}^{3/2}[1 - (1 - X)^{1/2}] + D_{po}\left(C - \frac{A}{B^2}\right)[1 - (1 - X)^{1/3}] + \frac{2A^2}{B^3}D_{po}^{1/2}[1 - (1 - X)^{1/6}]$$
$$+ \frac{2A^3}{B^4}\ln\left[\frac{A + BD_{po}^{1/2}(1 - X)^{1/6}}{A + BD_{po}^{1/2}}\right] + DX \tag{11}$$

$$C = \frac{\rho_p}{24C_o k_c}$$

$$D = \frac{N\pi\rho_p D_{po}^3}{72QC_o} = \frac{m_b}{12QC_o}$$

where X = fractional conversion $= 1 - (D_p/D_{po})^3$, and m_b = batch mass of carbon charged.

In applying equation (11), not only the properties of carbon and air but also the reaction rate constant as well as the probabilities of particle being in each region of the SB are necessary. The method for estimation of

these probabilities (p_a, p_f) has been illustrated in Part 1 of this paper (Tia *et al.*, 1991*b*). The combustion rate constant can be estimated from the correlation reported in the literature, and will be discussed later.

(ii) Nonisothermal particle model

The carbon particle temperature in this model is considered to change during combustion, and can be estimated from the unsteady energy balance:

$$\frac{\pi}{6}\rho_p C_{pp} D_p^3 \frac{dT_p}{dt} = \pi D_p^2 \left(\frac{1}{k_c} + \frac{D_p}{\mathrm{Sh}_i D_g}\right)^{-1} C_b H_c - Q_l \tag{12}$$

where subscript i represents the annulus, spout or fountain region, Q_l = heat loss from burning particle, and H_c = heat of combustion of the reaction $C + O_2 \rightarrow CO_2$. The values of Sh_i can be estimated from equations (8) and (9). For the annulus, the heat loss can be estimated from

$$Q_{l,a} = h_t(T_p - T_b) \tag{13}$$

and for the spout and fountain

$$Q_{l,i} = \frac{\mathrm{Nu}_i k_g}{D_p}(T_p - T_b) + \sigma\varepsilon_p(T_p^4 - T_b^4), \quad i = s, f \tag{14}$$

The estimation of total heat transfer coefficient h_t was illustrated in Part 1 (Tia *et al.*, 1991*b*), and Nu_i values are evaluated from (Ranz and Marshall, 1952)

$$\mathrm{Nu}_i = 2 + 0{\cdot}69\mathrm{Re}_i^{1/2}\,\mathrm{Pr}^{1/3}, \quad i = s, f \tag{15}$$

where Re_i is the Reynolds number in each region of spouted bed, as already defined in Part 1 (Tia *et al.*, 1991*b*).

The particle shrinkage rate at any time, therefore, can be estimated by combining equations (2)–(4), and changing Sh_b to Sh_i ($i = a, s, f$). The resulting expression is

$$-\frac{dD_p}{dt} = \left[\frac{N\pi\rho_p D_p^2}{24QC_o} + \frac{\rho_p}{24C_o k_c} + \frac{D_p}{\mathrm{Sh}_i D_g}\right]^{-1} \tag{16}$$

It is important to note that the implication of equation (16) is that all the N particles travel together from one region to the other. However this is unlikely to cause significant error because the residence times used in the model were based on the average values.

The fractional conversion X can be numerically estimated by starting from $t = 0$, $t_i = 0$, $D_p = D_{po}$, $C_b = C_o$, and $T_p = T_{po}$. The calculation steps are as follows:

(*a*) Estimate the particle residence times t_a, t_s, and t_f from the experimental value of t_c as described in Part 1 (Tia *et al.*, 1991*b*).
(*b*) Select the time step dt, and the time t_i is increased to $t_i + dt$.
(*c*) Calculate the new particle temperature T_p at time $t + dt$ from equation (12)–(15), and setting $\mathrm{Sh}_i = \mathrm{Sh}_a$ (equation (9)).
(*d*) Calculate the rate constant k_c from the known correlation (see the following Section) using the new T_p.
(*e*) Estimate a new D_p from equation (16) and a new C_b from equations (3) and (4) in which Sh_t and Sh_b are replaced by Sh_a from equation (9). The fractional conversion X then can be calculated from the new D_p and D_{po}.
(*f*) Check the time t_i to see whether it is equal to or greater than the residence time t_a of the particle in the annulus. If not, then repeat steps (*b*) to (*f*).
(*g*) If the time t_i is equal to or greater than t_a, then repeat steps (*b*) to (*e*) with $\mathrm{Sh}_i = \mathrm{Sh}_s$ (equation (8)) until the time t_i is equal to or greater than the particle residence time in the annulus and spout ($t_a + t_s$), after which go to the next step.
(*h*) Repeat steps (*b*) to (*e*) with $\mathrm{Sh}_i = \mathrm{Sh}_f$ (equation (8)) until the time t_i is equal to or greater than the particle cycle ($t_c = t_a + t_s + t_f$). At this time the particle completes one cycle. The time t_i is set equal to zero again.

(*i*) Calculate a new t_c from the new particle diameter at the end of the cycle (see Part 1, Tia *et al.*, 1991*b*), and repeat steps (*a*) to (*h*) for the next cycle and so on; the calculation stops when X is equal to the specific value selected.

(iii) Combustion kinetics

It is known that three regimes that have different controlling mechanisms can exist in char or carbon combustion (Turnbull *et al.*, 1984), namely, the kinetically controlled regime (regime I) where the combustion rate depends only on the intrinsic rates, the pore diffusion controlled regime (regime II) where the intraparticle diffusion is important, and the external diffusion controlled regime (regime III) where the process is controlled by oxygen diffusion from the surrounding gas phase. The important factors that determine the controlling mechanism for a given situation are temperature, particle size, relative velocity of the gas and particle, and pressure. In general, most researchers have tried to obtain data on the intrinsic chemical reaction rate by minimizing the effect of diffusion. This can be achieved by using a low pressure and/or low temperature, high velocity gas stream, and small particle size. However the analysis is still complicated owing to (Essenhigh, 1981) (i) the change in pore structure as the reaction proceeds, (ii) the presence of impurities which can promote or inhibit combustion reaction, (iii) the difficulties associated with the interpretation of BET data, and (iv) the effect of heat treatment on char reactivity. The experimentally determined values of combustion rate constants are therefore found to vary considerably, as summarized by Essenhigh (1981).

For first-order reaction, the rate constant based on external surface area as reported by Field *et al.* (1967) is used in this study

$$k_c = 59500 T_p \exp(-149227/R_g T_p) \text{ centimetres per second} \tag{17}$$

where $R_g = 8{\cdot}3143$ J/gmole K.

At low temperature, regime II combustion can occur if porous particles are used. Turnbull *et al.* (1984) showed that the combustion of a porous particle having a size generally greater than 1 mm, as found in an FB combustor, occurs in a thin porous layer near the particle surface for most of its life, and the first-order combustion rate constant based on the external surface can be expressed as

$$k_c = (k_i D_E S_E)^{0{\cdot}5} \tag{18}$$

where D_E = effective diffusivity of oxygen in porous solid, S_E = effective surface area for combustion, and k_i = intrinsic reaction rate constant based on pore surface area. The expression of k_i reported by Smith (1978) is

$$k_i = 2100 T_p \exp(-179400/R_g T_p) \text{ centimetres per second} \tag{19}$$

With these expressions of k_c, the fractional conversion X of carbon can be calculated from the model presented in Sections (i) and (ii) above.

EXPERIMENTAL DETAILS

The details of the experimental apparatus have been described elsewhere (Tia *et al.*, 1991*a*). Carbon samples were obtained from the carbon electrodes of dry cell batteries. They were first cut, and then ground to a nearly spherical shape using sand paper. Their equivalent diameter was indirectly determined by using the measured weight and density. To minimize the effect of small volatile content in the carbon samples, these were pyrolysed in a nitrogen atmosphere at 1123 K for 30 min. All the samples were oven dried for 24 h before testing. The apparent density of pyrolysed electrode carbon was 1·68 g/cm^3.

The bed was preheated under SFB mode to about 700 K, and then 2–3 g of 1–2 mm-diameter lignite particles were dropped batchwise into the bed from the top to increase its temperature, while the operation was changed to the selected mode and ratio of superficial velocity to the minimum spouting velocity (U/U_{ms} = 1·25). The bed preheating was continued to the desired temperature. As soon as the inventory of lignite

had burnt, a batch of monosize pyrolysed electrode carbon particles (8 g) was dropped into the bed and a stopwatch was started simultaneously. A chart recorder connected to an infrared gas analyser for off-gas measurement of carbon dioxide concentration was started just before the sample was dropped. The watch was stopped when glowing carbon particles were observed no longer, and the visually observed burnout time was obtained. Burnout times were also estimated from the off-gas concentration record shown in Figure 1. The burnout times obtained from these two methods differed by less than 10%. Carbon monoxide in off-gas was also checked in a separate experiment, and the measured concentration was found to be nearly zero. Therefore the complete combustion of carbon to CO_2 can be assumed.

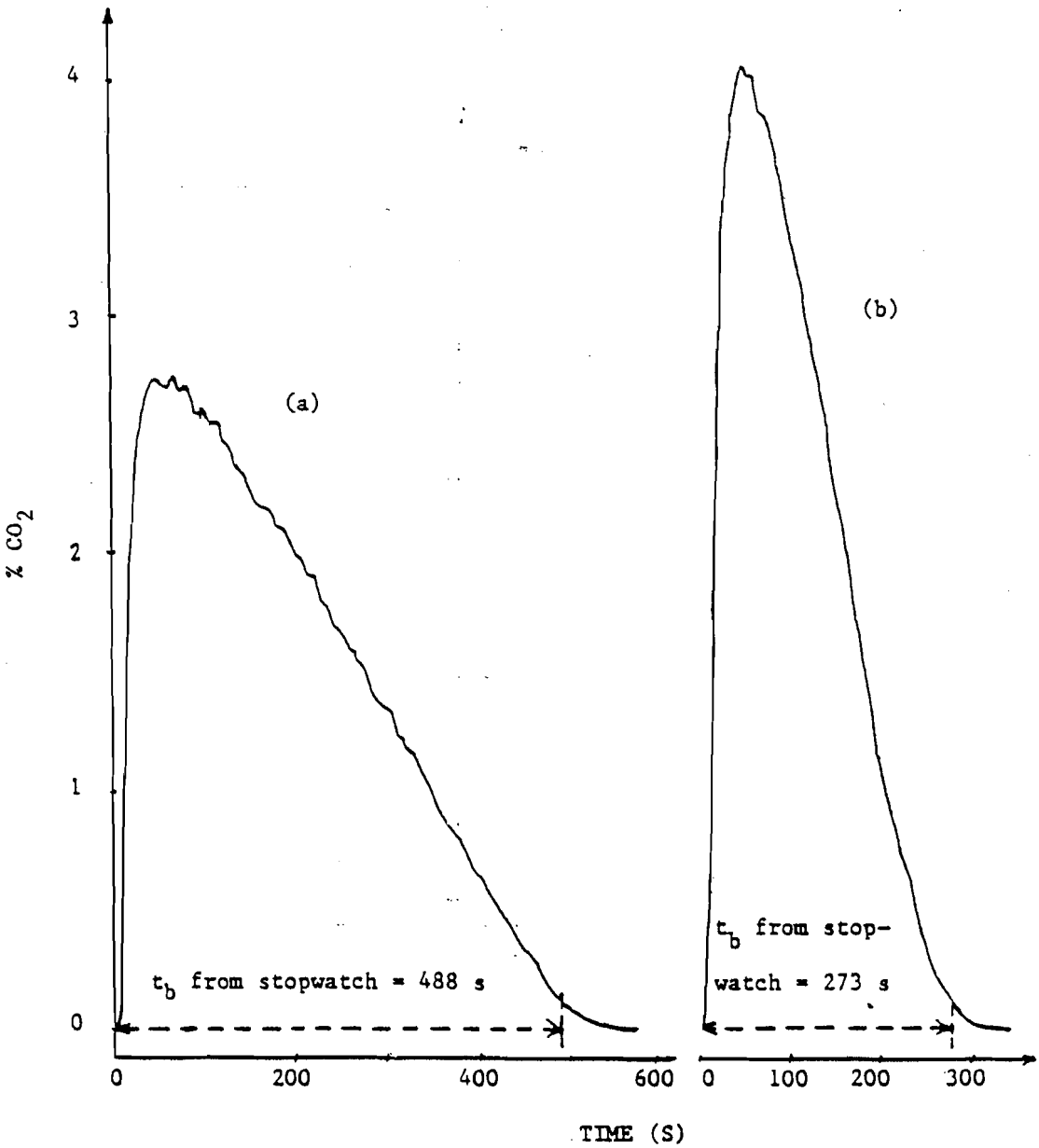

Figure 1. Concentration of carbon dioxide at outlet of laboratory-scale spouted bed combustor using carbon of (*a*) 4·07 mm diameter and (*b*) 2·37 mm diameter

RESULTS AND DISCUSSION

(i) Experimental results

The typical histories of carbon dioxide concentration in the exhaust gas for two different sizes of pyrolysed electrode carbon particle are shown in Figures 1*a* and *b*. The visually observed burnout times are also indicated in these Figures. Changing the bed temperature and batch mass gave nearly the same shape of curves with different burnout times and peak CO_2 concentration values. The time spent for the carbon dioxide concentrations to reach the maximum value was about 30–50 s. From visual observation, the ignition time delay was found to be 5–20 s, after which glowing combustion took place. Instead of showing a step increase in slope due to thermal ignition, the curves in Figure 1 show a gradual rise until the maximum. This corresponds to the theoretical analysis reported by Siemons (1987) that the thermal ignition of char in the FB combustors is a noncritical process, causing a gradual particle temperature rise without Semenov jump, with a gradual increase in the combustion rate. A decrease in the carbon dioxide concentration after the maximum can be attributed to the decrease in the surface area of the shrinking particles. It is important to note that, for the case of a large electrode carbon particle (4·17 mm or larger, Figure 1*a*), the curve in this period shows some fluctuation when compared with the smaller size (2·37 mm, Figure 1*b*). Since a batch of large particle size has fewer particles for a constant batch mass than the batch of particles of smaller size, it is dispersed less uniformly over the different regions of the SB (annulus, spout, and fountain). If most of the particles are in the annulus, in which the carbon particle temperature is low owing to the high rate of heat loss to inert sand, the combustion rate is low and the carbon dioxide concentration will drop. The concentration of carbon dioxide will increase if most of the particles are in the spout and fountain regions, in which the carbon particle temperature is high owing to the high oxygen mass transfer rate (high gas velocity) and low

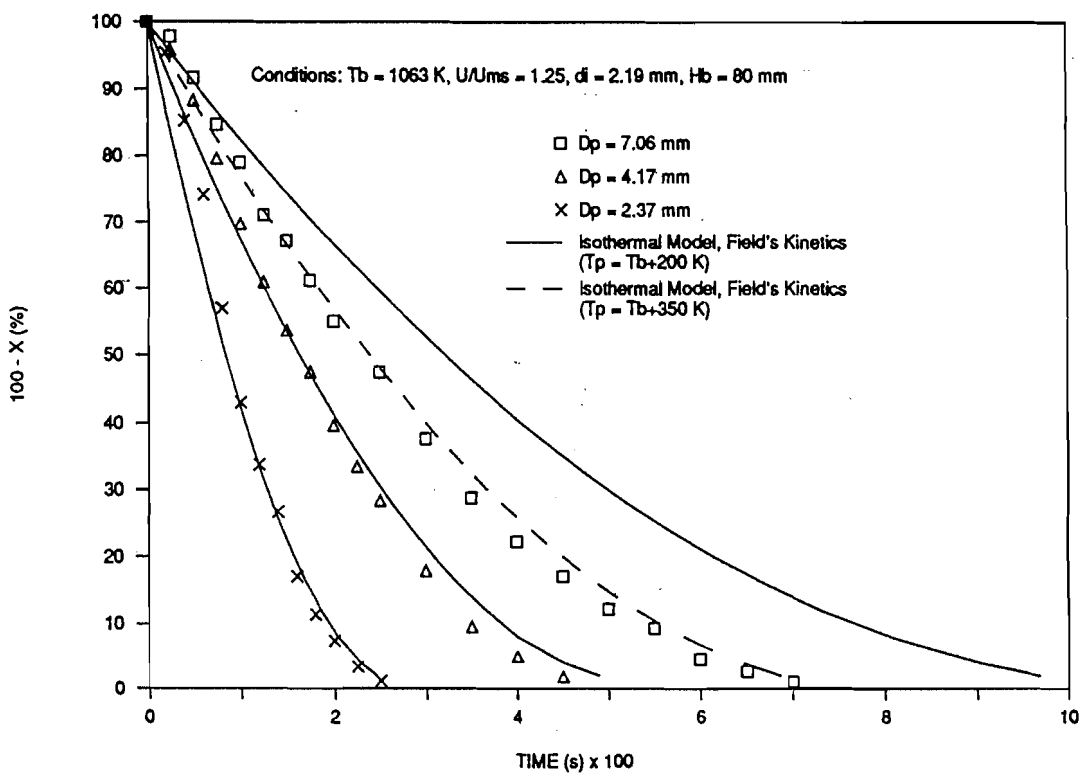

Figure 2. Effect of particle size on weight retained. Points are from experiment and lines are from isothermal particle model using Field *et al.* kinetics (regime I)

heat loss rate from the burning carbon particles. This behaviour is randomly repeated, so that the fluctuation of CO_2 concentration is observed.

The carbon conversion X at any time can be evaluated from the area under the carbon dioxide concentration curve. Figures 2 and 3 show the percentage weight of carbon retained (100-X) at different operating conditions. At a constant batch mass and bed temperature, the transient weight of small size carbon particles retained in the bed decreases more rapidly than the large ones (Figure 2). When the initial size of carbon particle and batch mass are kept constant, the transient weight retained for the case of low bed temperature decreases more slowly than at higher temperature (Figure 3).

Moreover, when the bed was operated under the spouting with aeration regime in SFB mode with the ratio of air flow through annulus to the total air flow rate (q/Q) of 0·2, the carbon burned faster than in the SB at the same condition (Figure 3). The result from this study is in contrast with that reported by Zhao *et al.* (1987*b*), who found that the burnout times of coal in an SFB operated under the jet-in-fluidized-bed regime is slightly longer than in the SB mode. The difference in hydrodynamic regimes under which the experiments were performed is presumed to compensate for the discrepancy. In this case the additional air flow in the annulus of the SFB, as reported by Donadono and Massimilla (1978), will promote the particle to pass the annulus–spout interface in the upper part of the bed. As a result, the probabilities of particles being in the spout and fountain regions are higher than those for an SB; this results, as mentioned earlier, in a higher combustion rate. For the same total gas flow rate, increasing the annulus gas velocity in the SFB also enhanced the combustion rate. At a high rate of conversion, where the particle size is small, the enhancement is greater owing to the long residence time of particles in the annulus.

(ii) Isothermal particle model

Using the properties of pyrolysed electrode carbon (Table 1), air properties for the gas phase, and the SB hydrodynamic correlations with inert sand properties as shown in Part 1 (Tia *et al.*, 1991*b*), the prediction of

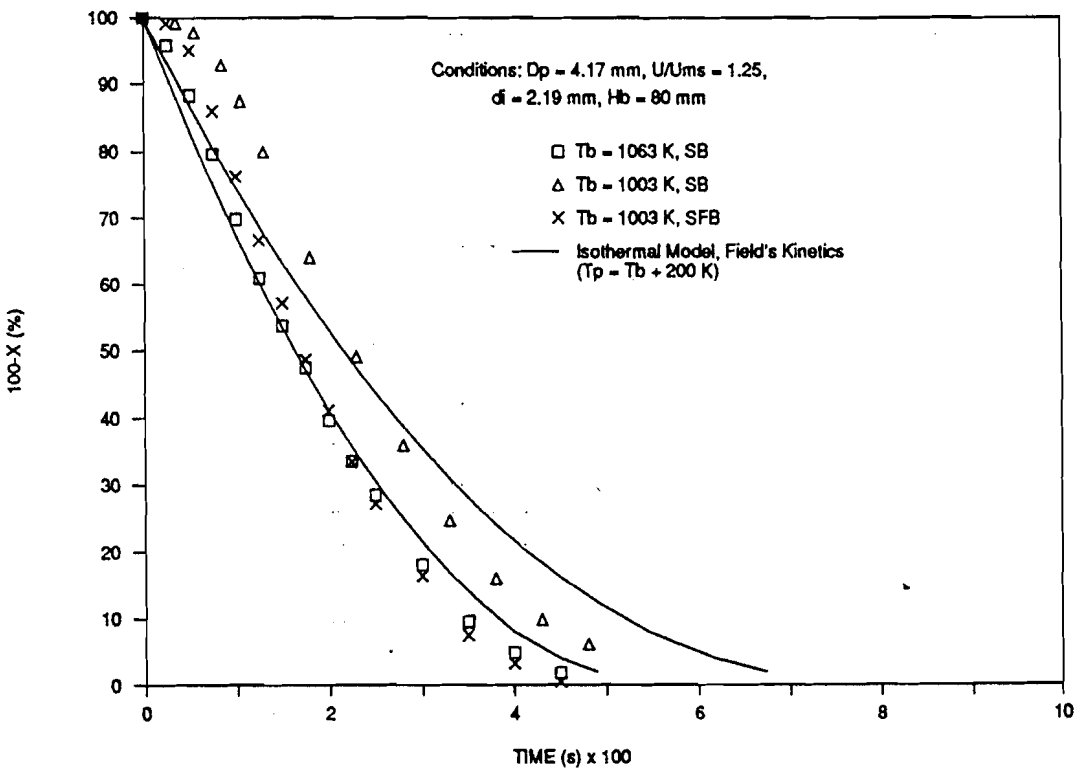

Figure 3. Effect of bed temperature and operation mode on weight retained. Points are from experiment and lines are from isothermal particle model using Field *et al.* kinetics (regime I)

Table 1. Thermal properties of pyrolysed electrode carbon and oxygen concentration used in model calculation

Pyrolysed electrode carbon	
Thermal conductivity, k_p, W/cm K[(a)]	= 0·0025
Specific heat, C_{pp}, J/g K[(b)]	= 0·702 for $T < 349$ K = 1·312 for $349 < T < 1165$ K = 1·618 for $T > 1165$ K
Emissivity, ϵ_p	= 0·8
Standard heat of combustion, H_c, J/gmole[(c)]	= 393,500
Apparent density, ρ_p, g/cm^3	= 1·68
Oxygen	
Oxygen concentration, C_o, gmole/cm^3	= $2{\cdot}363 \times 10^{-6}$ for $T_b = 1063$ K = $2{\cdot}504 \times 10^{-6}$ for $T_b = 1003$ K

(*a*) Ragland and Yang (1985), (*b*) Perry (1985), (*c*) Sharma and Mohan (1984)

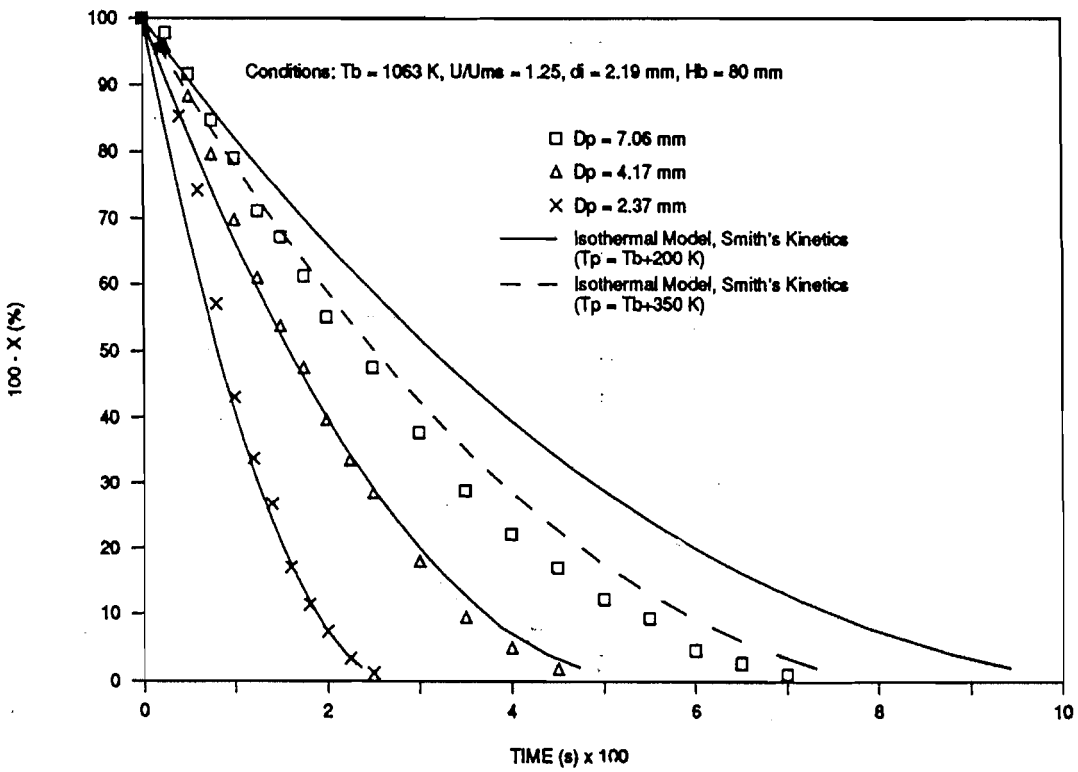

Figure 4. Effect of particle size on weight retained. Points are from experiment and lines are from isothermal particle model using modified Smith kinetics (regime II)

transient weight retained of carbon particles from the isothermal particle model is presented in Figures 2–3 and 4–5 for the Field *et al.* regime I and modified Smith's Regime II kinetics, respectively. The particle temperature was assumed to be 200 K higher than the bed temperature. Smith's kinetics (Smith, 1978) were modified by adjusting the pre-exponential factor to account for the uncertainties in the effective pore surface area S_E and the pore diffusivity of oxygen gas D_E. With the values of $S_E = 1{\cdot}28$ cm^2/cm^3 (Halder and Basu, 1987) and $D_E = 0{\cdot}5$ cm^2/s (Turnbull *et al.*, 1984), the adjusted pre-exponential factor that showed a good fit to

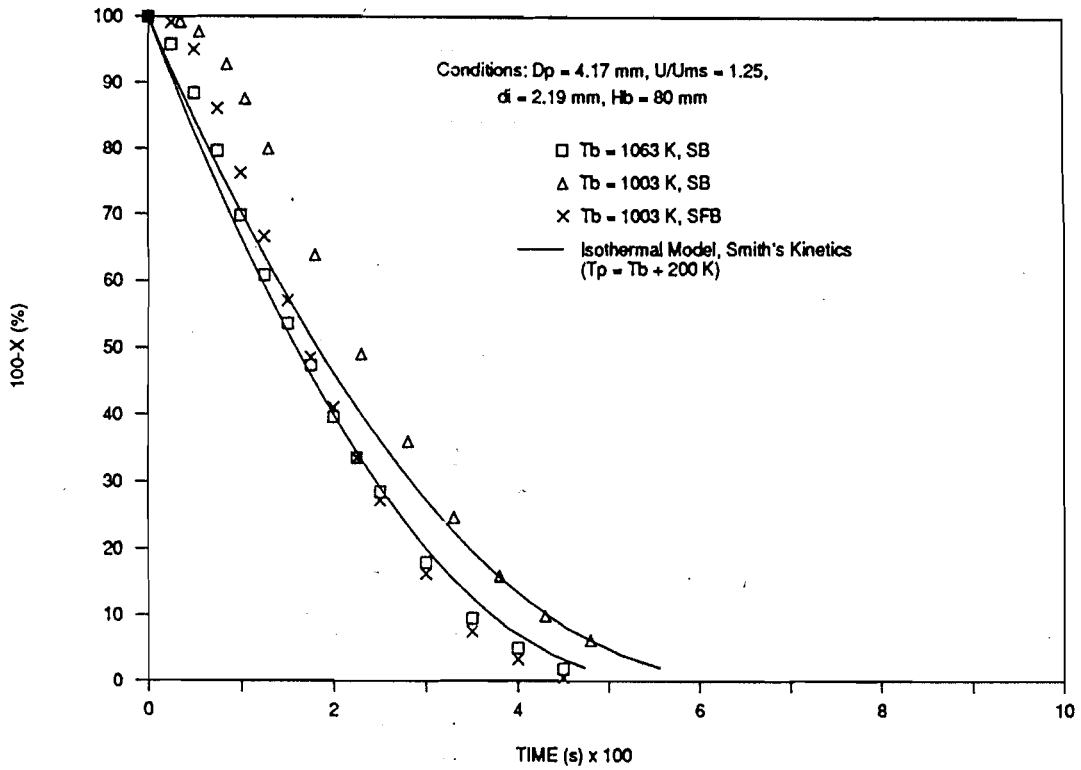

Figure 5. Effect of bed temperature and operation mode on weight retained. Points are from experiment and lines are from isothermal particle model using Smith kinetics (regime II)

the experimental data of $D_p = 4{\cdot}17$ mm and $T_b = 1063$ K was 1×10^6 cm/s K. This value was then used for the other conditions. The particle temperature in this study is assumed to be slightly higher than the typical assumed values in FB combustors, in which fuel particle temperature is 100–275 K above the bed temperature (Basu, 1977; Ross, 1979; Chakraborty and Howard, 1978 and 1981). As explained earlier, a higher fuel particle temperature is expected in an SB because of the high gas velocity and low heat loss rate in the spout and fountain regions.

Figures 2–5 show good agreement between experiment and theory except for large carbon particles and low bed temperature. However for all the studied conditions, significant underprediction at the beginning was observed. This can be attributed to the ignition time delay as well as the particle heating-up period, which have been neglected in this model.

At a high bed temperature (1063 K), slight overprediction at high conversion for 4·17 and 2·37 mm particles (Figures 2 and 4) was also observed. This may be due to the attrition effect, which is not considered in the model. From these results, the assumption of surface reaction for both regimes I and II using the kinetics of Field *et al.* and modified Smith, respectively, and isothermal particle temperature appears reasonable, at least for this bed temperature. Note that the case of modified Field *et al.* kinetics for regime II combustion (Turnbull *et al.*, 1984) was also calculated and gave nearly the same results as for regime I, and are not shown here. The reason for overprediction in the case of $D_p = 7{\cdot}06$ mm (Figures 2 and 4) for both Field *et al.* (regime I) and modified Smith (regime II) kinetics is due to the observed segregation of most of the large carbon particles at the bed surface near the annulus–spout interface. At this position, the particle temperature will be high because of the high oxygen transfer rate and the low heat loss from the burning particles to inert sand, so that the combustion rate is high. Therefore the weight of carbon retained in the bed, obtained from the experiment, is much lower than the prediction results. To check this postulate, the

assumed carbon particle temperature used in the model for this condition was increased up to 350 K above the bed temperature. The prediction results using either the Field *et al.* (regime I) or modified Smith (regime II) kinetics are in good agreement with experimental data; the combustion in this case approaches the diffusion control regime (regime III).

At a low bed temperature (1003 K), the predictions from both Field *et al.* (regime I) and modified Smith (regime II) kinetics give fairly good agreement compared to the experimental results (Figures 3 and 5). Significant underprediction was observed during the heating-up period (about 100–150 s) for both the rate expressions. The reason is that the particle temperature during this period is lower than the assumed value used in the theory, and hence the actual combustion rate is low. The other possible effect is the chance of oxygen gas to penetrate the carbon pore structure owing to the low combustion rate at low particle temperatures. Froberg and Essenhigh (1977) reported from their experiments using the ultrapure carbon that the internal burning can occur at a low particle temperature (< 1000 K), and the penetration depth increases when the carbon particle temperature decreases. Recently, Jung (1987) showed the occurrence of internal burning of petroleum coke in the low temperature (973–1073 K) FB combustor during the heating-up period. The internal burning during the heating-up period will, therefore, invalidate the assumption of surface combustion in the theory.

Since the equation of mean particle cycle time as a function of particle diameter was fitted in the exponential form (see Part 1, Tia *et al.*, 1991*b*), its value will approach infinity at zero diameter. Therefore equation (11), which gives the burnout time when the conversion is complete ($X = 100\%$), cannot be applied owing to the independence of constants A and B on the cycle time. The conversion of 98% is therefore used to represent the carbon burnout time. Comparison of burnout times recorded by a stopwatch for various initial particle diameters with the times for 98% conversion calculated from theory (Figure 6) showed good agreement for the small particle sizes. The overprediction due to the particle segregation, as discussed previously, is observed when the particle size is large. However, for a 7·06 mm particle and 1063 K bed

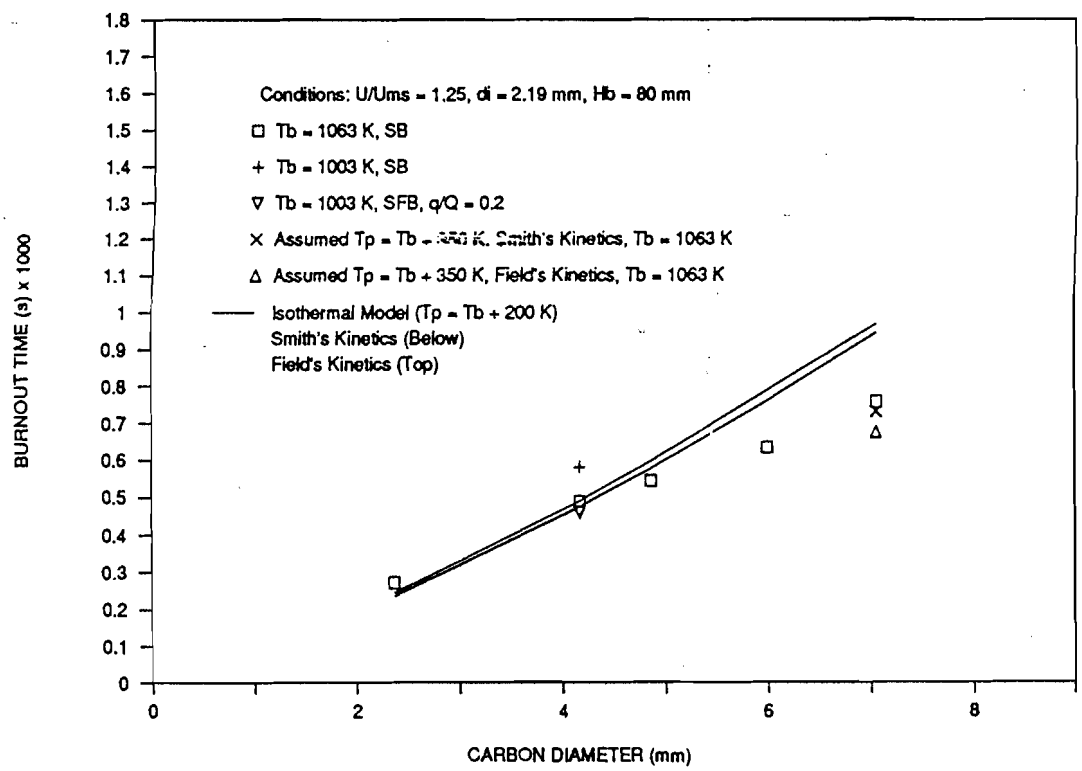

Figure 6. Comparison of experimental burnout times with isothermal particle model at various particle sizes

temperature, the predicted burnout times are close to the experimental values as shown in Figure 6, when the particle temperature is assumed to be 350 K higher than the bed temperature. Under the conditions studied, the predictions from equation (11) show that the chemical reaction term, $[DpC(1-(1-X)^{1/3})]$, and the last term, DX, contributed about 30–70% and 5–20% of the calculated burnout times, respectively. The rest is contributed by the remaining terms related to mass transfer.

(iii) Nonisothermal particle model

The comparison of nonisothermal model prediction using the information in Table 1, and Part 1 (Tia *et al.*, 1990*b*), and the Field *et al.* kinetics (regime I) with the experiment is shown in Figures 7 and 8, and Figures 9 and 10 show the comparison for modified Smith kinetics (regime II). As expected, during heating-up period, this model gave better results than the isothermal particle model.

At a high bed temperature (1063 K), the nonisothermal model with modified Smith kinetics showed good prediction for the particle sizes of 4·17 and 2·37 mm. However, the model gave notable overprediction for Field *et al.* kinetics. The explanation is that the rate derived from modified Smith kinetics (see equations (18) and (19) with a pre-exponential factor equal to 1×10^6 cm/s K) is more sensitive to temperature than the rate obtained from Field *et al.* kinetics (equation (17)). During heating-up, therefore, the reaction rate, and hence the particle temperature, remain low for a longer time in the model based on Field *et al.* kinetics (Figures 11–12). This leads to overprediction of weight retained owing to the cumulative effect. Moreover the internal burning during the heating-up period will invalidate the surface combustion assumed in the theory. Note that this overprediction was not observed in the isothermal model using Field *et al.* kinetics because of the compensation from the assumed particle temperature. In addition, the slightly underprediction for 2·37 mm particles at high conversion was also observed for the modified Smith expressions (Figure 9). This is

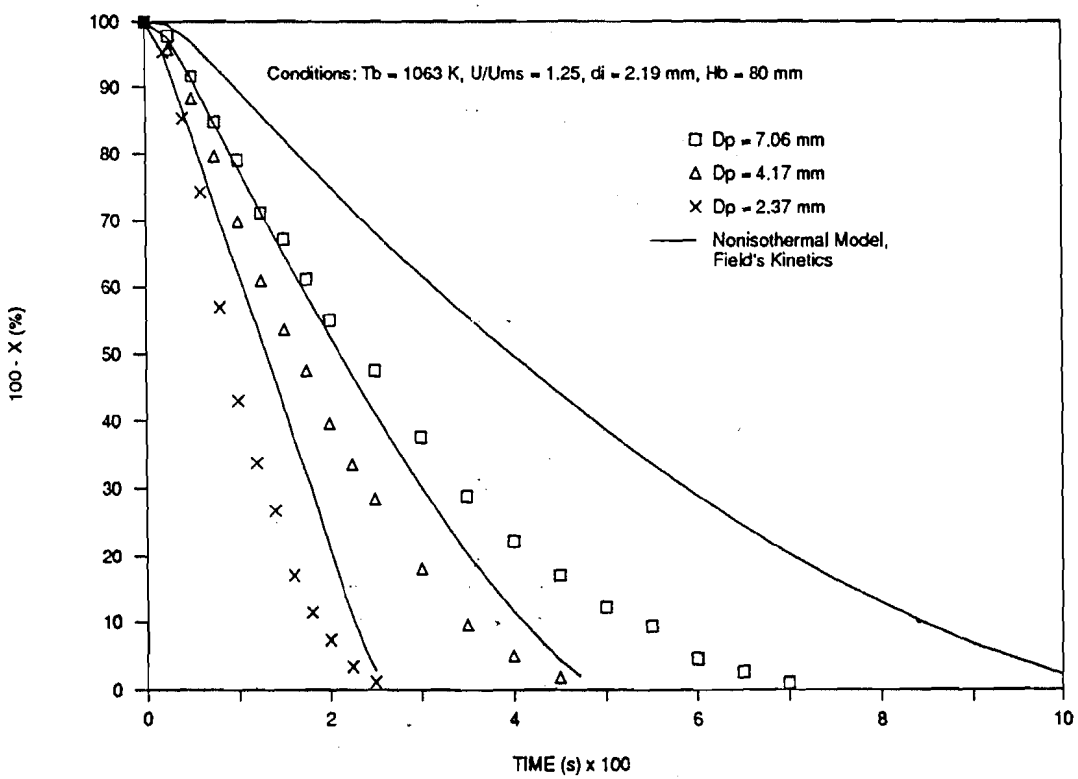

Figure 7. Effect of particle size on weight retained. Points are from experiment and lines are from nonisothermal particle model using Field *et al.* kinetics (regime I)

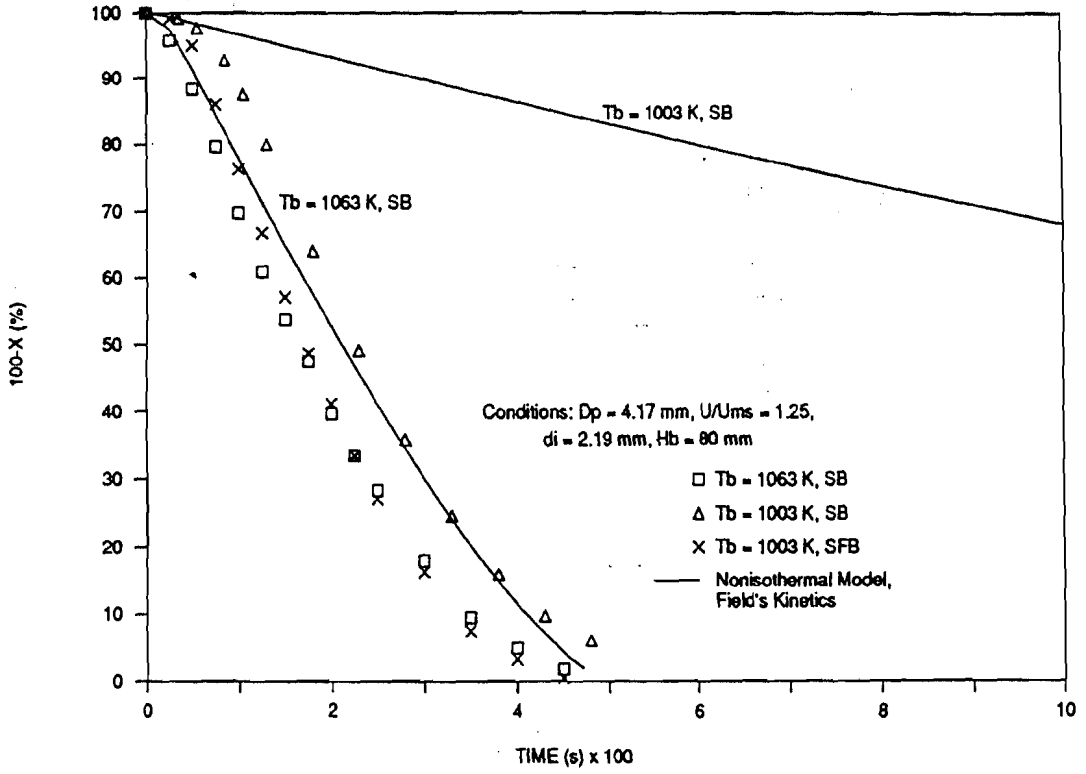

Figure 8. Effect of bed temperature and operation mode on weight retained. Points are from experiment and lines are from nonisothermal particle model using Field *et al.* kinetics (regime I)

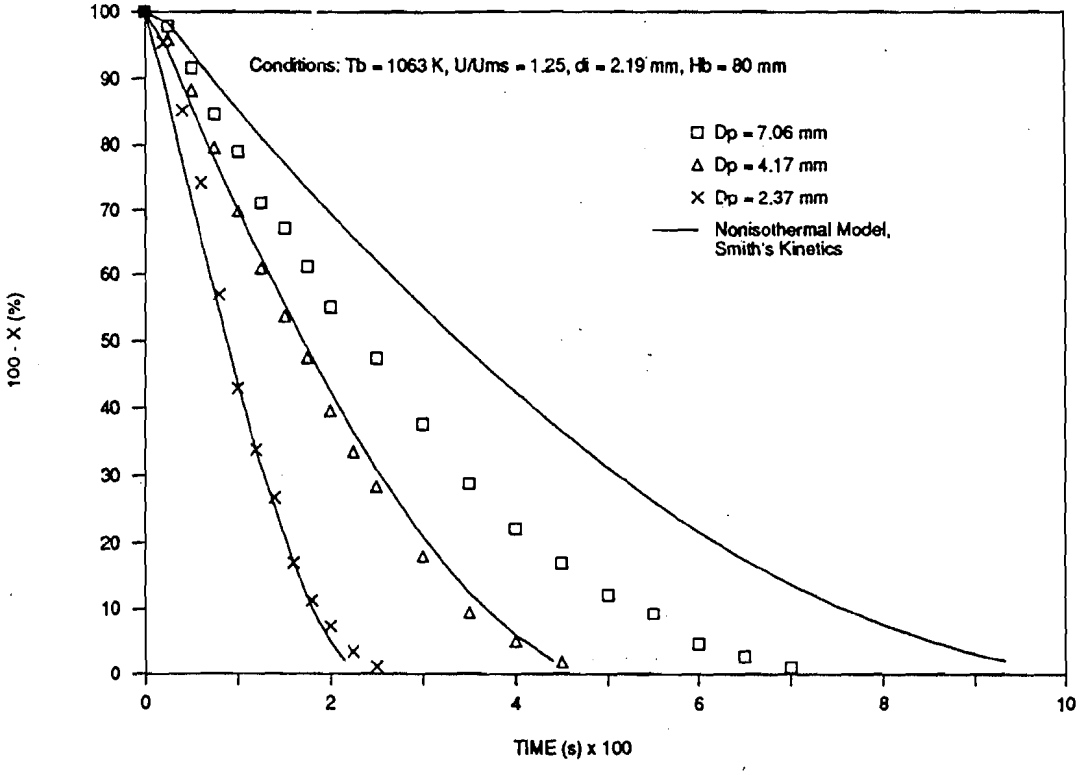

Figure 9. Effect of particle size on weight retained. Points are from experiment and lines are from nonisothermal particle model using modified Smith kinetics (regime II)

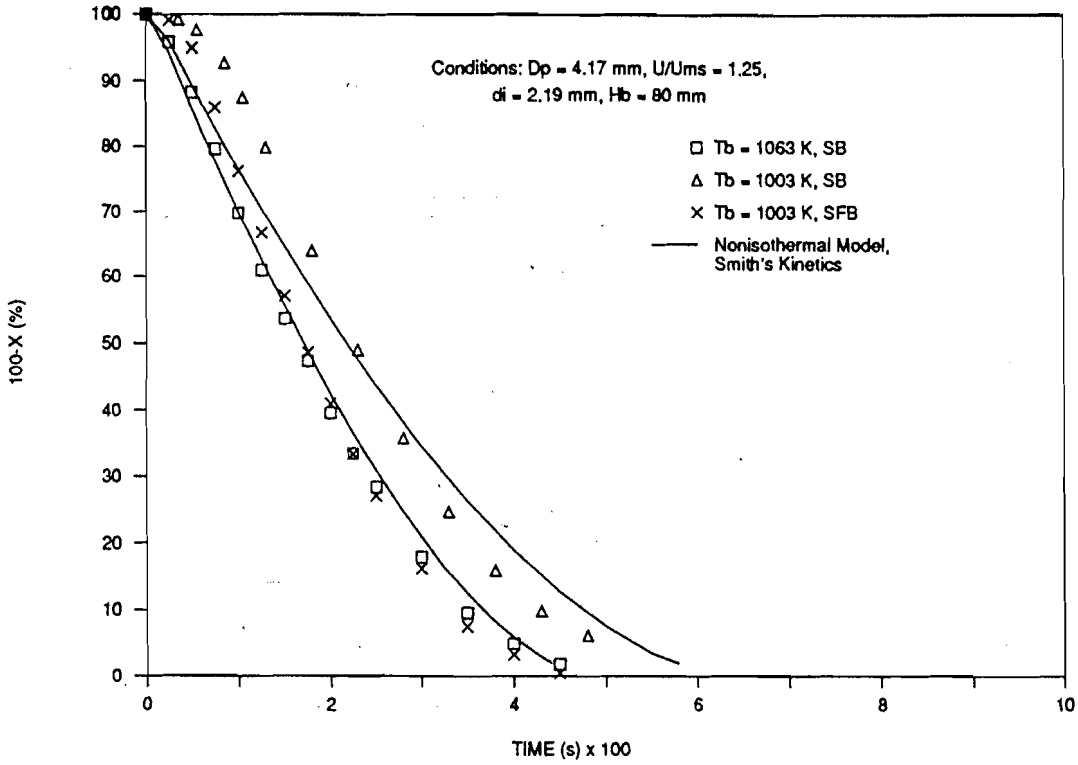

Figure 10. Effect of bed temperature and operation mode on weight retained. Points are from the experiment and lines are from nonisothermal particle model using modified Smith kinetics (regime II)

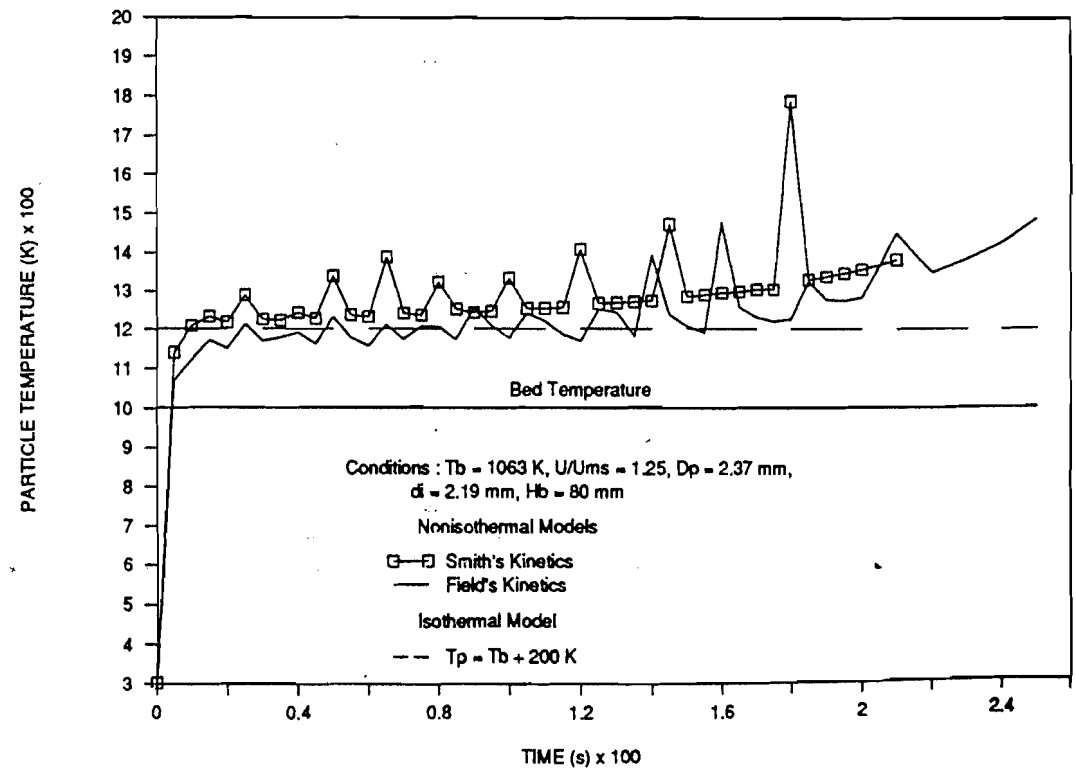

Figure 11. Comparison of 2·37 mm carbon particle temperatures from isothermal and nonisothermal particle models

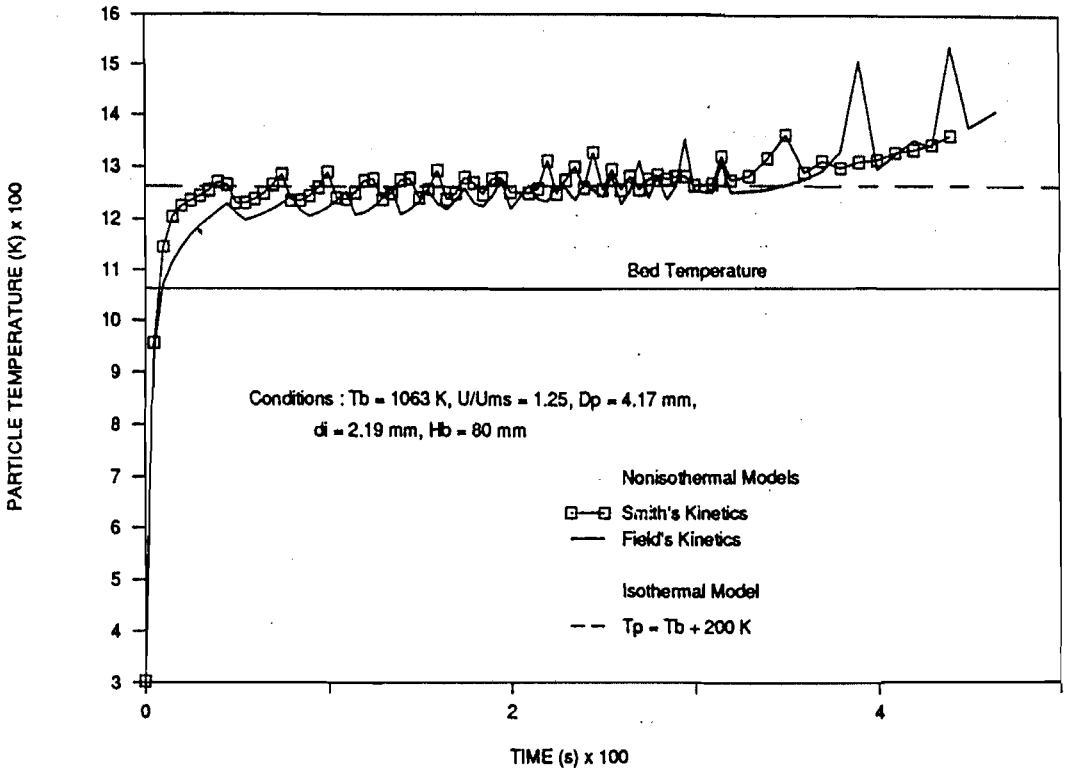

Figure 12. Comparison of 4·17 mm carbon particle temperatures from isothermal and nonisothermal particle models

due to the assumption that all the heat produced by the $C + O_2 \rightarrow CO_2$ reaction is used to heat the particles, leading to too high a particle temperature and combustion rate. This assumption is valid only for the relatively large size of carbon particle, because the combustion of CO produced by surface oxidation occurs in the gas phase close to the particle surface (Ross, 1979). The reaction radius of CO combustion, as derived by Ross (1979), increases when the particle size decreases. At high conversion, the particle size is small, therefore the heat of CO combustion may be dissipated by the inert sand rather than by raising the carbon particle temperature; and hence a lower combustion rate is found, compared with the theory. This effect is also presumed to compensate for the decrease in overprediction at high conversion of 2·37 and 4·17 mm particles for the case of Field *et al.* kinetics (Figure 7). In the case of 7·06 mm particle size, the segregation of carbon particles, as discussed earlier, causes significant overprediction for either rate expressions (Figures 7 and 9). Normally the segregation should be avoided in the SB combustor operation because it will create a hot spot, which can lead to instability of the bed resulting from the agglomeration of coal particles as well as to damage of the heat transfer area.

The variation of carbon particle temperature calculated from equation (12) is illustrated in Figures 11 and 12 for 2·37 and 4·17 mm particles, respectively. The particle temperature assumed in the isothermal model is also shown in these Figures as a reference (200 K higher than the bed temperature). For the 2·37 mm particle, both the rate expressions gave relatively high particle temperatures, especially at high conversion, when compared to the 4·17 mm particle or the isothermal case. This is due to the reason explained in the preceding paragraph. Note that the fluctuation of particle temperature calculated from this model is due to the difference in combustion rate in the different regions of the SB. The temperature of a 4·17 mm particle calculated from the nonisothermal model agrees well with the assumed value used in the isothermal model except near the beginning and the end of the burning period.

At a low bed temperature (1003 K), the Field *et al.* expression (equation 17) gave serious overprediction of the weight retained. This is due to the reason discussed above. Good agreement between the model prediction and experiment at high conversion was observed when the modified Smith expression was used (Figure 10).

Figure 13 presents the burnout times from a stopwatch in comparison with those calculated from the nonisothermal model using the Field *et al.* and modified Smith kinetics at 98% conversion. Because of the particle segregation, the overprediction at large particle sizes is observed, but the prediction for small particles shows good agreement with the experimental data. The slight underprediction observed for the case of small particles using modified Smith kinetics, as discussed above, is caused by the uncertainty of how much energy from CO combustion is transferred back to the particle.

(iv) Normalized weight/time history

In an SB combustor, the burnout time for batch experiment represents only the burnout of particles that spend a relatively long time in the annulus. This is in contrast with the developed models which are based on average values of particle cycle time. To overcome this problem, the experimental (from the carbon dioxide concentration curve) and theoretical values of the time required for 50% conversion have been used in the normalized weight/time plot. The typical results are shown in Figure 14. Both isothermal and nonisothermal models showed underprediction from the start to about 30% conversion. At high conversion, good prediction is obtained from the nonisothermal model using modified Smith kinetics. The discrepancies between the theory and experiment have been discussed in the preceding two Sections.

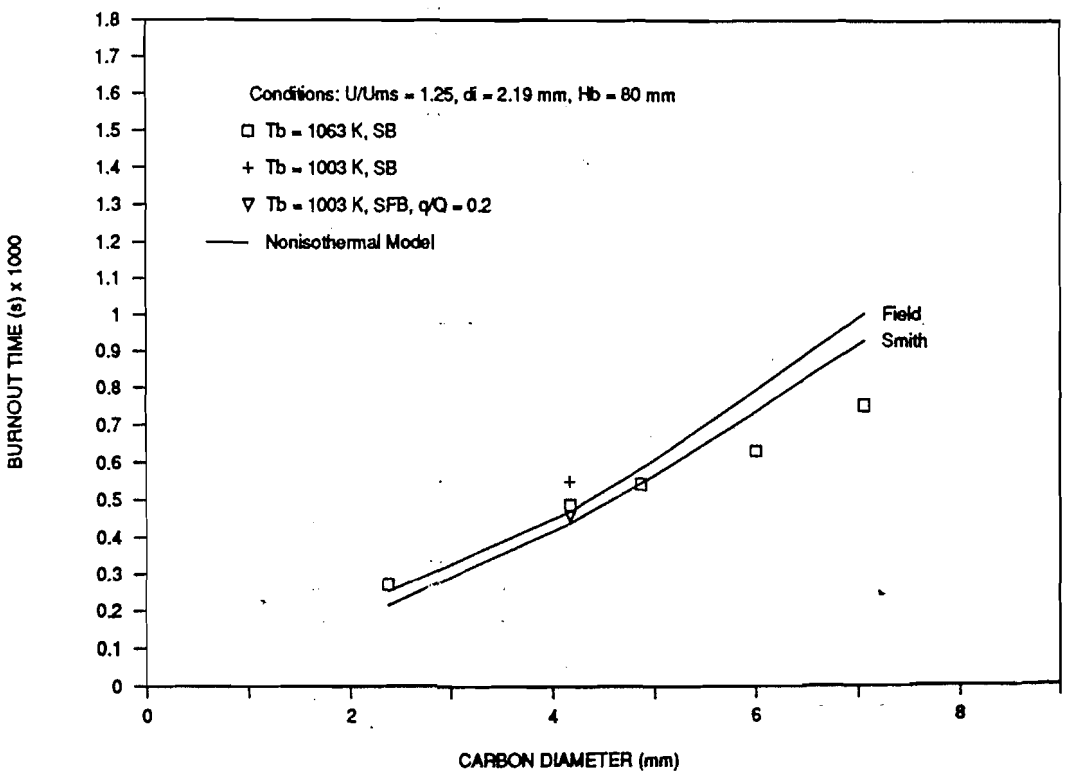

Figure 13. Comparison of experimental burnout times with nonisothermal particle model at various particle sizes

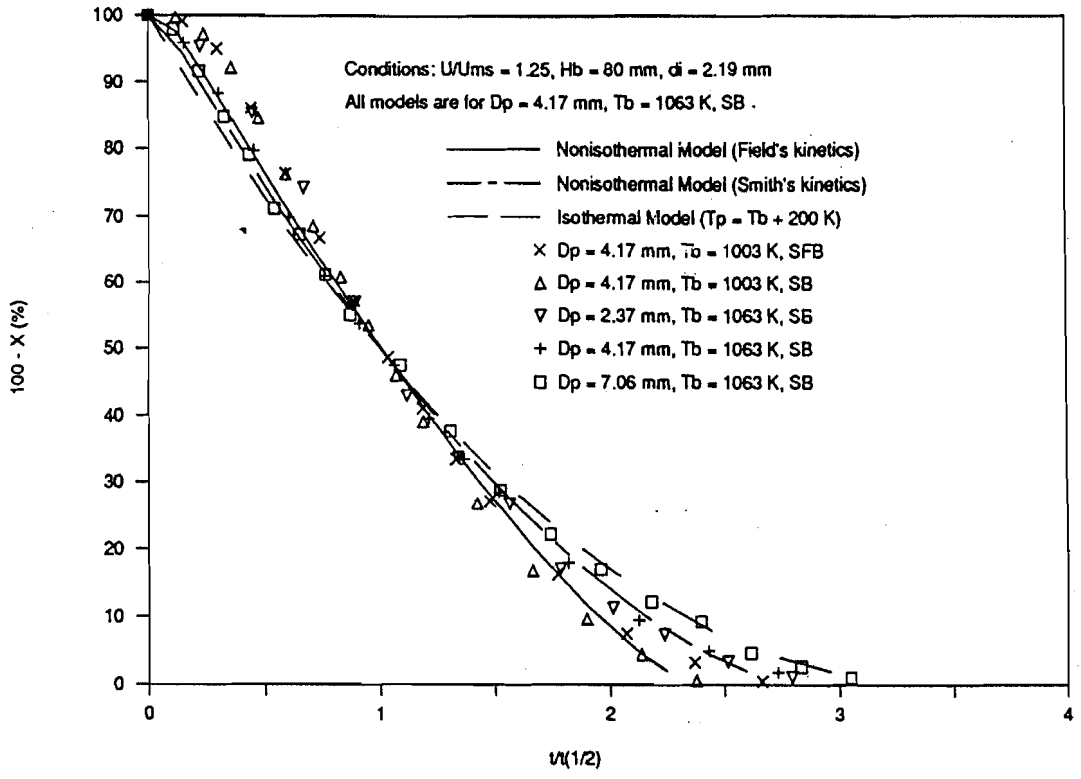

Figure 14. Normalized weight/time plot based on time at 50% conversion

CONCLUSIONS

Using the concept of residence times in the annulus, spout, and fountain, the batch combustion models of carbon particles in an SB combustor, for both the isothermal and nonisothermal particle, have been developed.

At a high bed temperature (1063 K), the prediction from both the models using the Field *et al.* (regime I) and modified Smith (regime II) kinetics with the assumption of surface combustion are in good agreement with the data taken from the laboratory-scale SB experiment. In the case of the isothermal particle model, the burning carbon particle temperature was assumed to be 200 K higher than the bed temperature. When the carbon particle used was large enough to cause the segregation, both models showed significant over-prediction for either rate expression.

Internal burning during the heating-up period and at low bed temperatures has a significant effect on the combustion kinetics used in the developed models. However, for low bed temperatures, the prediction from the nonisothermal model using modified Smith kinetics (regime II) with surface combustion is in good agreement with the experimental data, especially at high conversion.

NOMENCLATURE

A = cross-sectional area, cm^2
C = oxygen concentration, gmole/cm^3
C_p = specific heat, J/g K
D = diameter or diffusivity, cm(mm) or cm^2/s
E = activation energy, J/gmole
H = heat of combustion, J/g (J/gmole)

h = heat transfer coefficient, W/cm^2 K
K = combined rate constant (equation (4)), s^{-1}
k = chemical reaction rate constant or thermal conductivity, s^{-1} or W/cm K
k_d = mass transfer coefficient, cm/s
k_o = frequency or pre-exponential factor, s^{-1}
m_b = batch mass of carbon, g
N = number of particle
N_o = mass transfer flux of oxygen, gmole/s cm^2
Nu = Nusselt number
Pr = Prandtl number
p = probability
Q = gas flow rate, cm^3/s
Q_l = heat loss rate from the burning particle, W
q = gas flow rate at annulus inlet, cm^3/s
Re = Reynolds number
R_g = universal gas constant, J/gmole K
Sc = Schmidt number
Sh = Sherwood number
T = temperature, K
t = time, s^{-1}
U = superficial gas velocity, cm/s
u = interstitial gas velocity, cm/s
v = particle velocity, cm/s
X = fractional carbon conversion
ρ = density, g/cm^3
σ = Stefan–Boltzmann constant, J/K^4 cm^2
ν = kinematic viscosity, cm^2/s
λ = combustion mechanism factor (equation (4))
ω = combustion mechanism factor (equation (4))
ε = emissivity or void fraction

Subscripts

a = average value for annulus region
b = bed, or burnout condition
c = carbon, or cycle, or column
cc = combined conduction and convection between bed and coal particle
E = effective
e = exit
f = average value for fountain region
g = gas phase
i = intrinsic
o = bed inlet orifice or initial condition
p = particle
R = carbon surface
s = average value for spout region
t = total

REFERENCES

Basu, P. (1977). 'Burning rate of carbon in fluidized Beds', *Fuel*, **56**, 390
Chakraborty, R. K. and Howard, J. R. (1978). 'Burning rates and temperatures of carbon particles in a shallow fluidized-bed combustor', *J. Inst. Fuel*, **51**, 220

Chakraborty, R. K. and Howard, J. R. (1981). 'Combustion of char in shallow fluidized bed combustors', *J. Inst. Energy*, **54**, 48
Donadono, S. and Massimilla, L. (1978). 'Mechanism of momentum and heat transfer between gas jets and fluidized beds', *in* Davidson, J. F. and Keairns, D. L. (Eds) *Fluidization*, Cambridge University Press, 375
Essenhigh, E. H. (1981). 'Fundamentals of coal combustion', *in* Elliott, M. A. (Ed.) *Chemistry of coal utilization*, 2nd Suppl. Vol., John Wiley, New York, 1153
Field, M. A., Gill, D. W., Morgan, B. B. and Hawksley, P. G. W. (1967). *Combustion of pulverized fuel*, BCURA, Leatherhead, UK
Froberg, R. W. and Essenhigh, R. (1977). 'Reaction order and activation energy of carbon oxidation during internal burning', Proc. 16th Int. Symp. Combustion, Combustion Institute, Pittsburgh, 179
Halder, P. K. and Basu, P. (1987). 'The kinetic rate of combustion of electrode carbon in the temperature range of 1000–1200 K', *Canadian J. Chem. Eng.*, **65**, 696
Jung, K. (1987). 'Internal burning of petroleum coke particles in a fluidized bed', *Fuel*, **66**, 774
Khoe, G. H. and Weve, D. (1983). 'Visual observations of spouted bed gas combustion modes and their flow regimes', *Canadian J. Chem. Eng.*, **61**, 460
Kumpinsky, E. and Amundson, N. R. (1984). 'Reactor model assessment for the combustion of char in spouted beds of sand', *Industrial Eng. Chem.: Process Design and Development*, **23**, 784
La Nauze, R. D. and Jung, K. (1982). Proc. 19th Int. Symp. Combustion, Combustion Institute, Pittsburgh, 1087
Lim, C. J., Watkinson, A. P., Khoe, G. K., Low, S., Epstein, N. and Grace, J. R. (1988). 'Spouted, fluidized and spout-fluid bed combustion of bituminous coals, *Fuel*, **67**, 1211
Luss, D. and Amundson, N. R. (1969). 'Maximum temperature rise in gas-solid reactions', *AIChE J.*, **15**, 194
Perry, J. H., Ed., (1985). *Chemical engineer's handbook*, 6th Ed., McGraw-Hill, New York, USA
Rangland, K. W. and Yang, J. Y. (1985). 'Combustion of millimeter sized coal particles in convective flow', *Combustion and Flame*, **60**, 285
Ranz, W. E. and Marshall, Jr., W. R. (1952). 'Evaporation from drop, Parts I and II', *Chem. Eng. Progress*, **48**, 141 and 173
Ross, I. B. (1979). 'The efficiency of fluidized bed combustion', Ph.D. dissertation, University of Cambridge, UK
Siemons, R. V. (1987). 'The mechanism of char ignition in fluidized bed combustors', *Combustion and Flame*, **70**, 191
Sharma, S.P. and Mohan, C. (1984). *Fuels and combustion*, Tata McGraw-Hill, New Delhi
Smith, I. W. (1978). 'The intrinsic reactivity of carbon to oxygen', *Fuel*, **57**, 409
Tia, S. (1990). 'Combustion of lignite and carbon in spouted and spout-fluid beds', Ph.D. thesis, Energy Technology Division, Asian Institute of Technology, Bangkok, Thailand
Tia, S., Bhattacharya, S. C. and Wibulswas, P. (1991*a*). 'Combustion behaviour of coal and carbon in spouted and spout-fluid beds', *Int. J. Energy Research*, **15**, 249–255
Tia, S., Bhattacharya, S. C. and Wibulswas, P. (1991*b*). 'Spouted and spout-fluid bed combustors–1: Devolatilization and combustion of coal volatiles', *Int. J. Energy Research*, **15**, 185–201
Turnbull, E., Kossakowski, E. R., Davidson, J. F., Hopes, R. B., Blackshaw, H. W. and Goodyer, P. T. Y. (1984). 'The effect of pressure on the combustion of char in fluidized beds', *Chem. Eng. Research and Design*, **62**, 223
Zhao, J., Lim, C. J. and Grace, J. R. (1987*a*). 'Flow regimes and combustion behavior in coal-burning spouted and spout-fluid bed', *Chem. Eng. Sci.*, **42**, 2865
Zhao, J., Lim, C. J. and Grace, J. R. (1987*b*). 'Coal burnout times in spouted and spout-fluid beds', *Chem. Eng. Research and Design*, **65**, 426